Resolving tissue-level proteomic complexity in cutaneous squamous cell carcinoma (cSCC) with ultra high-plex spatial profiling

Rahul Ladwa
Princess Alexandra Hospital
Meg L Donovan
Wesley Research Institute
Naomi Berrell
Wesley Research Institute
Kidane Embaye
University of Queensland
Tony Blick
University of Queensland
Alexa E Lasley
Bruker Spatial Biology
Margaret L Hoang
Bruker Spatial Biology
Terence C Theisen
Bruker Spatial Biology
Joseph M Beechem
Bruker Spatial Biology
Chin Wee Tan
The Walter and Eliza Hall Institute of Medical Research
Arutha Kulasinghe
arutha.kulasinghe@uq.edu.au

University of Queensland

Short Report

Keywords:

Posted Date: December 10th, 2025

DOI: https://doi.org/10.21203/rs.3.rs-8245885/v1

Additional Declarations: Competing interest reported. Authors AEL, MLH, TCT, and JMB are employees of Bruker Spatial Biology. AK is on the Scientific Advisory Board for Omapix Solutions, Predxbio, Molecular Instruments and Visiopharm. All other authors declare no financial or non-financial competing interests.

Abstract

Immune-checkpoint inhibitors (ICIs) are the primary treatment for advanced cutaneous squamous cell carcinoma (cSCC). Tumour microenvironment differences between immunocompetent and immunocompromised patients may underpin the development of effective biomarkers. Across 4 cSCC patients, we profiled 190 consecutively gridded, pathology assigned, regions of interest, using the GeoMx Discovery Protein Atlas (1116 protein markers). Expression profiles underscored by metabolic and immunological activity, including type I interferon signalling, differentiate patient immune competency.

Main text

Cutaneous squamous cell carcinoma (cSCC) is one of the most common cancers worldwide, with a predilection for the head and neck region due to its high UV-radiation exposure[1]. The incidence of skin cancers is rising with rates > 100 per 100,000 in North America and Europe, escalating to 2,875/100,000 among males over 60 years in Australia[2]. Advanced cSCC commonly develop in immunocompromised patients[3], with solid organ transplant recipients having a 65-to-250 times higher incidence of cSCC [4,5]. While most cSCCs in immunocompetent patients follow an indolent course with excellent disease-specific survival, immunosuppression, whether from solid-organ transplantation, haematological malignancy, or autoimmune disease therapies, worsens prognosis. Due to its association with cumulative solar damage, cSCC has an exceptionally high tumour mutational burden (TMB, 45 mutations/Mb)[6] translating to increased neoantigen production, which underpins sensitivity to ICI therapy. Multiple clinical trials of ICI targeting the PD-1/PD-L1 axis have demonstrated responses in approximately 50% of recurrent/metastatic or locally advanced cSCC for which no curative local treatment options are available[7]. While a clinical ICI trial that included cSCC patients with haematological malignancies found comparable efficacy[8], real world analysis suggest patients with haematological malignancies experience worse progression free and overall survival following ICI therapy[9]. Understanding the tumour microenvironment (TME) between immunocompromised and immunocompetent populations is paramount for risk stratification, treatment selection and development of tailored surveillance strategies.

Here, we applied discovery focussed, ultra high-plex spatial proteomics with sequencing readout to profile 1116 protein markers, including 5 IgG controls and 5 housekeeper proteins, (GeoMx Digital Spatial Profiler (DSP), GeoMx Discovery Proteome Atlas - DPA, Bruker Spatial Biology, US) for regions across the tumour, stroma, and tumour-stroma interface from whole-slide cSCC tissue sections (Fig. 1). Our study profiled 190 gridded consecutive regions of interest (ROIs) across 4 patient baseline (pre-treatment) tissue biopsies of cSCC. Tissue biopsies of 4 patients with inoperable, advanced cSCC were collected, consisting of 2 immunocompetent and 2 immunocompromised patients (Fig. 1A). We used a pathology-informed grid based spatial region selection strategy (Fig. 1B) to map the spatial interface between the tumour and stroma regions of the samples, where Hematoxylin and Eosin (H&E) staining (Fig. 1C, top) was paired with the GeoMx DPA profiling (Fig. 1C, bottom).

The data were processed using the quality control (QC) pipeline from the R package, StandR[10]. As expected, correlations between the control markers were weak (Figure S1A), and the mean expressions of IgG and housekeeper controls were at the low and high ends of the protein expression range, respectively (Fig. 1D). Protein markers like EGFR, CD8, CD68 and CD4 are all well placed above background signals (Fig. 1D). In order to use transcriptome-based data analysis tools, each protein (isoform) marker was mapped to its corresponding gene/transcript via NCBI annotations.

QC involved assessment of sample and protein quality, with no protein markers removed, 2 ROIs removed based on nuclei counts and library sizes (Figure S2A), and slide effects identified to be confounding the data. The count data was batch corrected for effects of slides using the R package *RUV4* (k = 3) with both "AOI segmentation" and "regions/segments of interest" factors of interest to keep (Figure S2B). After adjustment, the tumour and stroma samples were well separated across PC1 and interface and non-interface samples segregated/separated within either the tumour or the stroma samples on the PCA plots (Fig. 2A). Differential expression (DE) analysis was then performed using previously developed pipelines optimised for GeoMx DSP spatial proteomic data[11,12] to elucidate proteins related to spatial locations in the TME (tumour, stromal and interface regions).

Looking at differences between tumour and stroma samples broadly (Figure S4), we observed enrichment of DNA mismatch repair and tricarboxylic acid (TCA) cycle gene sets in the tumour samples and an enrichment of autophagy gene sets in the stroma samples. These pathways reflect characteristic hallmark features of cancer, namely cellular attempts to repair mutated DNA and metabolic activity, while the stroma regions are potentially under metabolic stress regulation and homeostasis via autophagy. Furthermore, lower CD4 and CD68 expression in the tumoral regions is suggestive of an immune excluded environment.

When comparing between tumour regions, we found an enrichment of growth and proliferation related PDGF, EGF and TGFβ gene sets in the immunocompetent patients, while the immunocompromised patients are enriched in lipid and fatty acid metabolic process and interferon (IFN) type 1 gene sets (Fig. 2B). On the other hand, in the comparison of the stroma samples, immunocompetent patients have enrichment in gene sets related to energy metabolism and post-transcriptional regulation of gene expression while immunocompromised patients have enriched gene sets for type I IFN production (Fig. 2B). Of note, within the stromal and tumoural regions of the immunocompromised patients, we see an elevated expression of TREX1, a gene that regulates the removal of unwanted DNA and prevents immune activation[13].

We then interrogated the protein expression profiles of samples at the tumour-stroma interface against central tumour and stromal regions (Fig. 2C). Within the tumour compartment, the interface regions appear to be enriched in FGF/FGFR-mediated signalling and lipid and fatty acid metabolism gene sets while regions away from the interface, more central to the tumour bulk, had elevated mitochondrial aerobic respiration and ATP production. For the stroma region, stromal interface ROIs had enriched MAPK signalling regulating fatty acid biosynthesis and metabolism while the central stromal regions had

gene sets linked with the regulation of protein metabolism and degradation, as well as immune surveillance via antigen processing.

The ability to measure hundreds to thousands of proteins with spatial resolution on single slides can be transformative for translational cancer research. Traditionally, only a few biomarkers can be measured from tissue samples in a clinically relevant timeframe. In this study, we present discovery plex (> 1,000 proteins) profiling of cSCC and the integrated analysis of the proteomic profiles between regions in the TME across immunocompetence statuses in cSCC. The GeoMx DPA assay provides high-plex proteomic readout, with the ability to generate quantifiable protein data within a few days, allowing for the characterization of molecular and functional differences within the TME.

In this proof-of-concept study, we measured and characterized the complex TME in cSCC. Our findings from this study highlight biologically relevant compartment-specific protein expression and subsequently used this to infer enriched genesets in tumour and stroma regions of cSCC samples. We identified tumour regions to have increased metabolic activity, whilst the stroma regions were maintaining homeostasis via autophagy and metabolic stress regulation[14]. Typically, autophagy indicates the deletion of mutated mitochondria and is commonly considered an antitumour behaviour that can be a response to decreased ATP generation or oxidative stress[15]. These findings indicate a metabolic cross talk between tumour and stromal regions. Specifically, tumoral TCA upregulation has been found to induce an oxidative stress environment within stromal regions, due to the secretion of reactive oxygen species from tumour cells[16]. Furthermore, the non-tumour cells within the TME must adapt to survive in nutrient depleted and/or harsh environments[17].

A carefully considered ROI selection can provide more spatial insight into the TME dynamics. We demonstrate that pathology-informed ROI selection is beneficial to better describe the spatial landscape of tissues, as evident by the identification of differences in metabolic activity closer to the tumour-stroma interface. The importance of ROI selection and the adoption of spatial readout is particularly apparent when we inspect the interface and central/non-interface regions for tumour and stromal regions independently. In both cases, we saw dysregulated metabolic pathways within the interface regions while there was more stable energy utility in the central regions. These findings support prior research that points to increased growth, proliferation, metastatic capacity, and metabolic activity in peripheral tumour cells, especially in more aggressive tumours[18]. In this study, upregulated lipid metabolism was found at the interface and this supports previous studies where lipid metabolism was vital for tumour growth and proliferation[19]. Similarly, we see dysregulated metabolism in the non-tumour interface, which may be co-evolution mechanisms enabling non-tumour cells to exist and adapt to the changing nutrient availability and TME conditions[17]. The power of this approach is apparent when comparing clinical covariates, such as immunocompetency status. For instance, the proteomic profile of immunocompetent patients was driven by oncogenes like TFGβ and PDGF[20,21], while the immunocompromised groups featured activation of type 1 IFN, known to contribute to T cell exhaustion, and where chronic activation may have a role for predicting ICI treatment resistance[22].

This study has a few limitations. Firstly, to demonstrate the utility of this assay and application for translational research, we profiled a sub-cohort of cSCC whole slide tissues. Whilst we profiled a relatively large area by gridding across the entire tissue section to cover tumour, stromal and interface regions, the number of patient samples was limited. To address this, we envisage expanding this study to a larger cohort of cSCC in the future. Secondly, the resolution of the assay provides high-plex discovery proteomics with ROI or AOI resolution, which can range from tens to hundreds of cells in the area profiled, providing a multi-cellular spatial resolution. This does however position the assay towards using a pathology-informed ROI/AOI selection strategy to compare across cell types/histologies of interest in a targeted fashion.

This study demonstrates the utility of ultra high-plex spatial proteomic profiling of the cSCC TME. This assay could provide an avenue to identify biomarkers associated with clinical endpoints, such as progression free survival or overall survival. In our proof-of-concept study, we found a concerted immune-related activation signature in immunocompromised patients and differing metabolic profiles between immune status.

Methods

Patient cohort

This study has Metro South Health Human Research Ethics Committee (MSH HREC) study approval (LNR/2020/QMS/66612) and University of Queensland Human Research Ethics ratification. All patients provided written informed consent. Tissues were collected retrospectively from the Princess Alexandra Hospital from cSCC patients where tissue blocks were accessible for spatial analysis. Pathology Queensland prepared serial sections and performed hematoxylin and eosin (H&E) staining, pathology review and provided specimens for tissue analysis.

H&E and pathology annotations

Whole Slide Images (WSIs) stained with Hematoxylin and Eosin (H&E) were manually annotated by a pathologist using QuPath software (version 0.6.0-rc4)[23]. Annotation was done manually by delineating regional boundaries to define specific histological features apparent on the WSIs. Each WSI was systematically examined at multiple magnification levels to ensure precise identification and segregation of tissue elements.

Within each region, histological features were rigorously annotated by tracing various tissue compartments including tumour, stromal areas, immune cell infiltrations or lymph nodes, blood vessels, normal tissue and artifactual areas. This multilayered annotation approach provided comprehensive spatial mapping of the tissue architecture to capture both morphological and microenvironmental diversity. Annotations were exhaustively applied across the entirety of each WSI to maximize spatial coverage, enabling robust quantitative and qualitative analyses.

GeoMx (Bruker Spatial Biology, US) sample preparation

Slides were prepared using a modified, manual version of the GeoMx DPS Spatial Proteogenomics Assay protocol described in MAN-10158-05-01 which allows for profiling of both ultra-high plex GeoMx RNA and Protein assays on the same slide in a single acquisition. Briefly, slides were baked at 60°C for 30 minutes, dewaxed using xylene, and dried in 100% and 95% Ethanol Washes. For epitope retrieval, slides were submerged in heated Leica Bond ER2 solution and placed in a pressure cooker at 100°C for 20 minutes on the low-pressure setting. The slides were digested for 15 minutes at 37°C in a 0.1 µg/mL Proteinase K solution and then fixed with 10% NBF for 5 minutes. After two five-minute washes in Tris-glycine solution, GeoMx WTA RNA probes were added to the slides before an overnight incubation in a 37°C hybridization oven. The following morning, the slides went through two rounds of a 2xSSC/50% formamide stringent wash. In preparation for the additional of the protein panels, the slides were washed with 1X TBS-T for 5 minutes. The Protein Probe Mix, comprised of a developmental build of the GeoMx Discovery Proteome Atlas and the CD45 and PanCK morphology markers, was made following the manufacturer's recommendation and added to the slides. Slides with the Protein Probe Mix were incubated at 4°C overnight in a humidity chamber. The next morning slides were washed three times for 10 minutes in 1X TBS-T and then fixed with 4% PFA for 30 minutes at room temperature. The DNA dye, Styo13, was included on the slides for 15 minutes and after two brief washes with TBS-T, the slides were loaded on a GeoMx instrument for ROI selection and acquisition.

Library preparation and sequencing

DSP collection plates were dried down and then each collection well was resuspended in 10 µL of water. Libraries from the RNA probes were generated using 4 µL from the DSP collection wells and Seq Code primers. 74 µL of water was added to the remaining volume in the DSP collection plates and then 4 µL of this diluted mix was used with Pro Code primers to generate the libraries for the Protein probes. Libraries were first pooled equally by analyte type and then mixed at a 2:1 ratio of the protein to the RNA libraires. PhiX at 1 nM was added to the combined library and then loaded into an Illumina P4 cartridge and run on an Illumina Next Seq 2000 sequencer.

GeoMx DSP (Bruker Spatial Biology, US) proteomic analysis

The data for the GeoMx DPA were measurements of protein abundance of 1116 proteins including 5 housekeeping proteins (Histone H3, GAPDH, RPS6, Calreticulin and TOMM20) and 5 background control (Rat IgG2a, Mouse IgG2b, Hamster IgG, Rabbit IgG, and Mouse IgG1) probes. The computational analyses pipelines conducted are as per previously established for the GeoMx IPA (Immuno-oncology Proteome Atlas) data[11] with modifications.

Pre-processing, quality control and normalization

The probe normalised protein (probeQC) counts of each ROI were imported for pre-processing, quality control, and normalisation that were conducted using modifications based on the standR[12] pipeline. Protein expression, sample metadata, and clinical information were integrated into one data structure. Proteins (isoforms) were also mapped to their respective gene/transcript via NCBI annotations (Homo Sapiens Genome assembly GRCh38 r110). Initial QC assessment included investigating correlations between housekeeping and background control proteins expression (logCPM). Protein level QC was conducted using either *edgeR::filterByExpr* or *standR::addPerROIQC*, filtering out low expressing proteins with less than 5 counts per sample in more than 90% of the samples. Sample QC filters out low expression ROIs, in this case filtering out 2 outlier ROIs where protein expression depth < 180,000 per ROI and nuclei count > 400 cells per ROI. Relative log expression (RLE) plots and principal component analysis (PCA) across ROIs were utilised to identify factors associated with biological variations or technical variations (batch effects). A clear slide /sample effect was observed. To correct for this, standR's *findNCGs* function was used to identify 200 top negative control proteins (NCPs) based on the identified batch factor. The *RUV4* function from the *ruv* R package[24] was then utilised via standR:: geomxBatchCorrection function using the NCPs and the factor k = 3 to batch correct. The result of the corrections was assessed using the RLE and PCA of the adjusted count data.

Differential expression (DE) analysis.

DE analysis was performed using the *edgeR[25] (v4.6.1)* and *limma* (v3.64.0) R packages[25,26]. As mentioned earlier, protein isoforms were translated to the corresponding genenames/ID to utilise the gene based statistical packages. DE was modelled using linear models with experimental, clinical, and biological factors using an empirical Bayes approach, which estimates the common and gene wise variation to model each gene's variation while borrowing information from all other genes. The linear model was then fitted to appropriate experimental designs using the *limma-voom-eBayes* pipeline via *edgeR::voomLmFit* function with duplicate correlation and sample weights to first estimate the consensus correlation across patient and account for patient variation as a random effect[27] and second to estimate empirical sample quality weights for each sample. The contrasts of interest were then applied using *limma::eBayes* function to assess differential expression. The Benjamini–Hochberg procedure was applied for multiple testing adjustments based on an adjusted $p < 0.05$. The contrasts of interest include A) between tumour and stroma regions, B) immuno-competent vs immuno-compromised and C) interface vs non-interface regions.

Gene-set Enrichment Analysis (GSEA)

GSEA uses the statistics from DPA's DE analysis. Gene sets from the Molecular Signatures Database's (MsigDB) Hallmarks, C2 (curated gene sets), C5 (Ontology gene sets) and C7 (immunological signature gene sets) categories were tested against the dataset using a rotational geneset testing approaching with the *limma::fry* function. Pathways and terms from the Kyoto Encyclopedia of Genes and Genomes (KEGG) pathway database were assessed using the *limma*::*kegga* function and gene ontology (GO)

enrichment was investigated using the *limma::goana* function. A false discovery rate (FDR) < 0.05 threshold were used to define significance. The results from GSEA were inputted into the vissE (1.16.0)[28] R package where clusters of enriched gene sets with common biological themes were identified and visualized as bar plots alongside GSEA statistics.

Declarations

Data availability

The protein data generated in this study from the GeoMx DPA is available at https://doi.org/10.48610/7078364.

Code availability

All code for data cleaning and analysis associated with the current submission is an application of publicly available R packages, which are disclosed in within *Methods*. Any additional information required to reanalyse the data reported in this paper is available from the lead contact upon request.

Acknowledgments

This study was supported by Metro South Health (MSH) and the Princess Alexandra Research Foundation (PARF). The authors would like to acknowledge the Wesley Research Institute. We thank Christine Kang, Ashley Heck, Alyssa Rosenbloom, and Michael Rhodes for their contributions to the study during their time at Bruker Spatial Biology.

Author contributions

Concept: JMB, AK, RL

Experimental: MLD, KE, AEL, MLH, TCT, RL

Analysis: TCT, CWT

Writing and critical review: MLD, NB, TB, RL, CWT, AK, KE, AEL, MLH, TCT, JMB

Funding

This study was funded by Metro South Health (MSH) and the Princess Alexandra Research Foundation (PARF). The funder played no role in study design, data collection, analysis and interpretation of data, or the writing of this manuscript.

Competing Interests

Authors AEL, MLH, TCT, and JMB are employees of Bruker Spatial Biology. AK is on the Scientific Advisory Board for Omapix Solutions, Predxbio, Molecular Instruments and Visiopharm. All other authors

declare no financial or non-financial competing interests.

References

1. Urban K, Mehrmal S, Uppal P, Giesey RL, Delost GR. The global burden of skin cancer: A longitudinal analysis from the Global Burden of Disease Study, 1990–2017. JAAD International 2021;2:98–108. DOI: https://doi.org/10.1016/j.jdin.2020.10.013.
2. Wilson A, Goltsman D, Nankervis J, Clark J, Gupta R, Ashford B. Defining the incidence of cutaneous squamous cell carcinoma in coastal NSW Australia. Australasian Journal of Dermatology 2022;63(2):213–216. DOI: https://doi.org/10.1111/ajd.13830.
3. Pham JP, Staeger R, Joshua AM, et al. An updated review of immune checkpoint inhibitors in cutaneous oncology: Beyond melanoma. European Journal of Cancer 2025;214. DOI: 10.1016/j.ejca.2024.115121.
4. Alhamad T, Venkatachalam K, Linette GP, Brennan DC. Checkpoint Inhibitors in Kidney Transplant Recipients and the Potential Risk of Rejection. Am J Transplant 2016;16(4):1332–3. (In eng). DOI: 10.1111/ajt.13711.
5. Lailheugue A, Gibier JB, Lassailly G, Truant S, Pruvot FR, El Amrani M. Primary squamous cell carcinoma of the peristomal skin of gastrostomy in a transplant patient: a first case report. J Gastrointest Oncol 2019;10(3):573–576. (In eng). DOI: 10.21037/jgo.2019.01.05.
6. Gupta R, Strbenac D, Satgunaseelan L, et al. Comparing Genomic Landscapes of Oral and Cutaneous Squamous Cell Carcinoma of the Head and Neck: Quest for Novel Diagnostic Markers. Mod Pathol 2023;36(8):100190. (In eng). DOI: 10.1016/j.modpat.2023.100190.
7. Hughes BGM, Guminski A, Bowyer S, et al. A phase 2 open-label study of cemiplimab in patients with advanced cutaneous squamous cell carcinoma (EMPOWER-CSCC-1): Final long-term analysis of groups 1, 2, and 3, and primary analysis of fixed-dose treatment group 6. J Am Acad Dermatol 2025;92(1):68–77. (In eng). DOI: 10.1016/j.jaad.2024.06.108.
8. Lang R, Welponer T, Richtig E, et al. Nivolumab for locally advanced and metastatic cutaneous squamous cell carcinoma (NIVOSQUACS study)-Phase II data covering impact of concomitant haematological malignancies. J Eur Acad Dermatol Venereol 2023;37(9):1799–1810. (In eng). DOI: 10.1111/jdv.19218.
9. Leiter U, Loquai C, Reinhardt L, et al. Immune checkpoint inhibition therapy for advanced skin cancer in patients with concomitant hematological malignancy: a retrospective multicenter DeCOG study of 84 patients. J Immunother Cancer 2020;8(2) (In eng). DOI: 10.1136/jitc-2020-000897.
10. Liu N, Bhuva DD, Mohamed A, et al. standR: spatial transcriptomic analysis for GeoMx DSP data. Nucleic Acids Research 2024;52(1):e2-e2.
11. Tan CW, Berrell N, Donovan ML, et al. The development of a high-plex spatial proteomic methodology for the characterisation of the head and neck tumour microenvironment. npj Precision Oncology 2025;9(1):191. DOI: 10.1038/s41698-025-00963-0.

12. Liu N, Bhuva DD, Mohamed A, et al. standR: spatial transcriptomic analysis for GeoMx DSP data. Nucleic Acids Research 2023;52(1):e2-e2. DOI: 10.1093/nar/gkad1026.
13. Zhou W, Richmond-Buccola D, Wang Q, Kranzusch PJ. Structural basis of human TREX1 DNA degradation and autoimmune disease. Nature Communications 2022;13(1):4277. DOI: 10.1038/s41467-022-32055-z.
14. Li A, Gao M, Liu B, et al. Mitochondrial autophagy: molecular mechanisms and implications for cardiovascular disease. Cell Death & Disease 2022;13(5):444. DOI: 10.1038/s41419-022-04906-6.
15. Filomeni G, De Zio D, Cecconi F. Oxidative stress and autophagy: the clash between damage and metabolic needs. Cell Death & Differentiation 2015;22(3):377–388. DOI: 10.1038/cdd.2014.150.
16. Martinez-Outschoorn UE, Balliet RM, Rivadeneira DB, et al. Oxidative stress in cancer associated fibroblasts drives tumor-stroma co-evolution: A new paradigm for understanding tumor metabolism, the field effect and genomic instability in cancer cells. Cell Cycle 2010;9(16):3256–76. (In eng). DOI: 10.4161/cc.9.16.12553.
17. Kimmelman AC, Sherman MH. The Role of Stroma in Cancer Metabolism. Cold Spring Harb Perspect Med 2024;14(5) (In eng). DOI: 10.1101/cshperspect.a041540.
18. Jiménez-Sánchez J, Bosque JJ, Jiménez Londoño GA, et al. Evolutionary dynamics at the tumor edge reveal metabolic imaging biomarkers. Proceedings of the National Academy of Sciences 2021;118(6):e2018110118. DOI: doi:10.1073/pnas.2018110118.
19. Kook E, Kim DH. Elucidating the Role of Lipid-Metabolism-Related Signal Transduction and Inhibitors in Skin Cancer. Metabolites 2024;14(6) (In eng). DOI: 10.3390/metabo14060309.
20. Loos B, Salas-Bastos A, Nordin A, et al. TGFβ signaling sensitizes MEKi-resistant human melanoma to targeted therapy-induced apoptosis. Cell Death & Disease 2024;15(12):925. DOI: 10.1038/s41419-024-07305-1.
21. Hosaka K, Yang Y, Seki T, et al. Pericyte-fibroblast transition promotes tumor growth and metastasis. Proc Natl Acad Sci U S A 2016;113(38):E5618-27. (In eng). DOI: 10.1073/pnas.1608384113.
22. Holicek P, Guilbaud E, Klapp V, et al. Type I interferon and cancer. Immunol Rev 2024;321(1):115–127. (In eng). DOI: 10.1111/imr.13272.
23. Bankhead P, Loughrey MB, Fernández JA, et al. QuPath: Open source software for digital pathology image analysis. Scientific Reports 2017;7(1):16878. DOI: 10.1038/s41598-017-17204-5.
24. Johann A. Gagnon-Bartsch LJ, Terence P Speed. Removing Unwanted Variation from High Dimensional Data with Negative Controls. Tech Reports California: Berkeley, University of California, 2013 2013.
25. Chen Y, Chen L, Lun ATL, Baldoni PL, Smyth GK. edgeR 4.0: powerful differential analysis of sequencing data with expanded functionality and improved support for small counts and larger datasets. bioRxiv 2024:2024.01.21.576131. DOI: 10.1101/2024.01.21.576131.
26. Ritchie ME, Phipson B, Wu D, et al. limma powers differential expression analyses for RNA-sequencing and microarray studies. Nucleic Acids Res 2015;43(7):e47. (In eng). DOI: 10.1093/nar/gkv007.

27. Robinson MD, McCarthy DJ, Smyth GK. edgeR: a Bioconductor package for differential expression analysis of digital gene expression data. Bioinformatics 2010;26(1):139–40. DOI: 10.1093/bioinformatics/btp616.

28. Bhuva DD, Tan CW, Liu N, et al. vissE: a versatile tool to identify and visualise higher-order molecular phenotypes from functional enrichment analysis. BMC Bioinformatics 2024;25(1):64. DOI: 10.1186/s12859-024-05676-y.

Figures

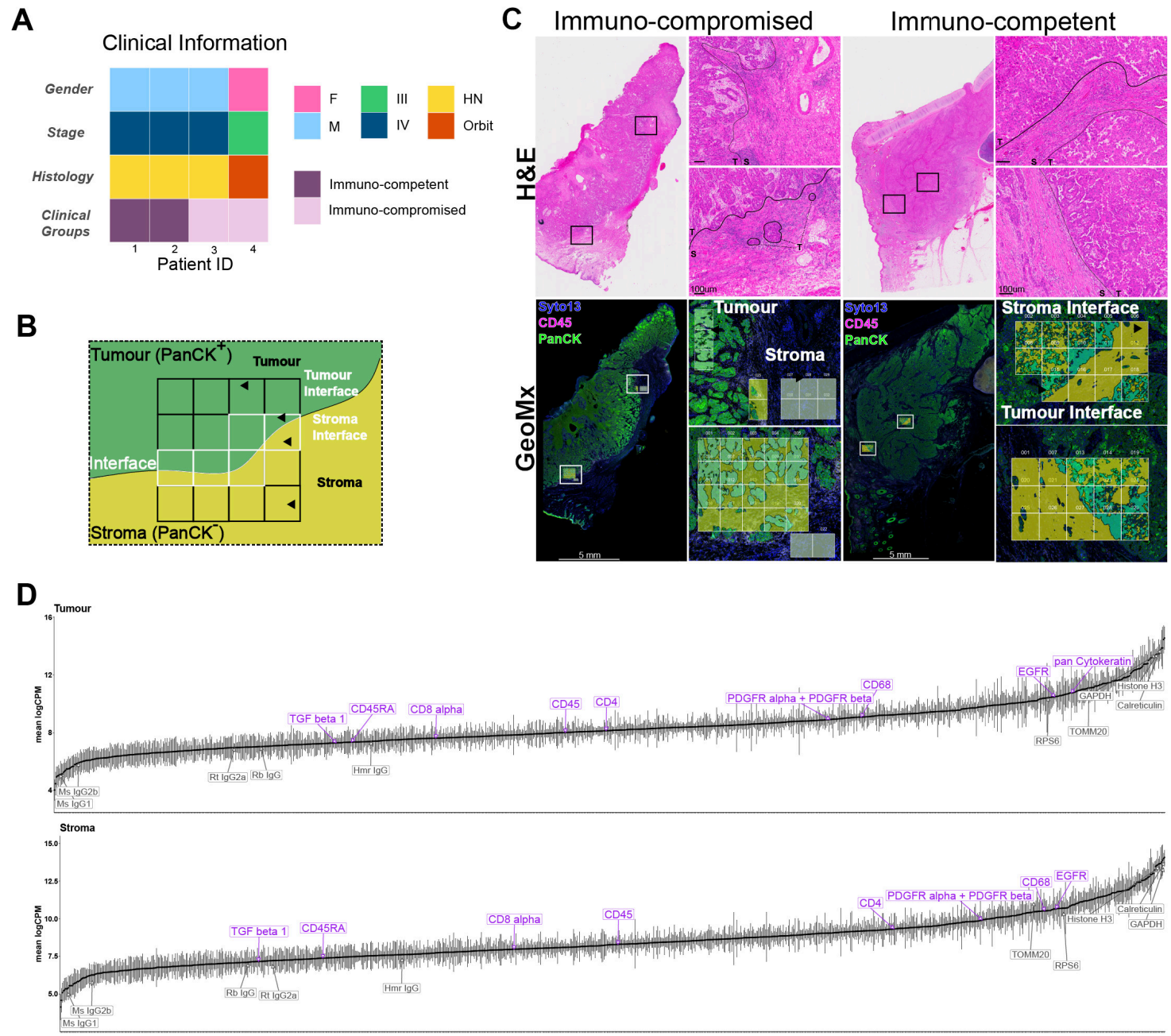

Figure 1

Overview of study. (A) Clinical information of the 4 cSCC patients that were profiled with GeoMx Discovery Proteome Atlas (DPA, Bruker Spatial Biology, US). (B) 190 gridded consecutive regions of interest (ROIs) were selected across the 4 patients, capturing tumour, stroma, and interface regions. (C) Representative images of same slide H&E and GeoMx DSP staining of 2 patients (1 immuno-compromised and 1 immuno-competent) showing ROI placement. (D) Mean marker expression plot for tumour (top) and stroma (bottom) ROIs with IgG controls and housekeepers labelled grey and selected markers labelled in purple.

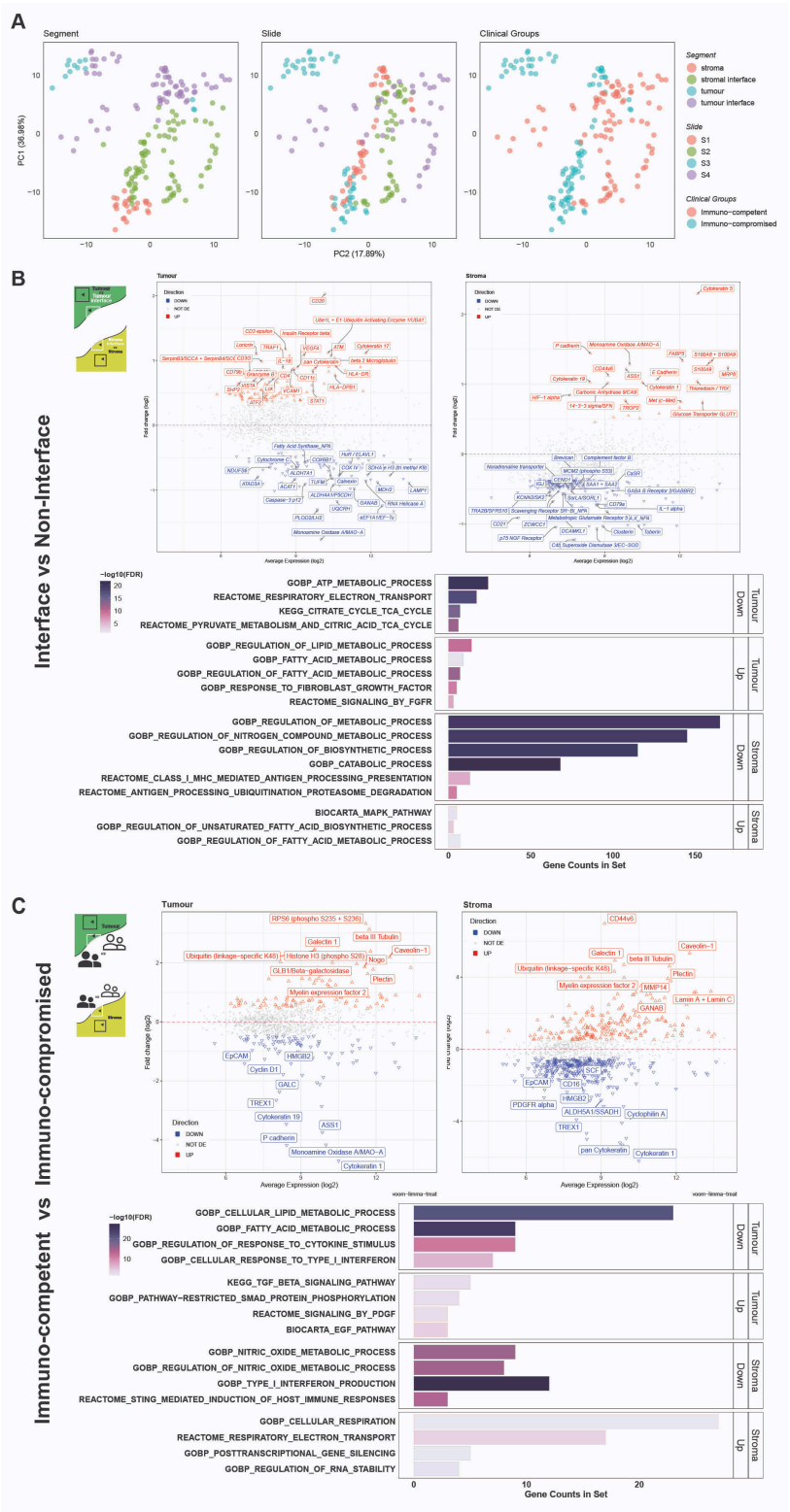

Figure 2

Data quality assessment, DE and pathway analysis. **(A)** PCA plots of batch corrected (*RUV4* k=3) data, stratified by factors segment, slide (i.e. patients) and clinical groups, indicating that segmentation variations are accounted for by PC1 and PC2 while patient/slide effects were reduced. **(B-C)** DE analysis results presented as M (log ratio)-A (mean average) plots and top enrichment pathways as geneset-DE genes counts bar plots for (B) Interface (Up) vs non-interface (Down) in tumour or stroma samples and (C) Immuno-competent (Up) vs immuno-compromised (Down) in tumour or stroma samples. *Limma-voom* eBayes pipeline used in the DE analysis with DE markers identified using a cutoff based on an adjusted p-value of ≤ 0.05 using the Benjamini Hochberg procedure. *Limma::fry*function used for the pathway enrichment analysis, providing the gene counts in each gene-set and associated FDR

Supplementary Files

This is a list of supplementary files associated with this preprint. Click to download.

- DPAbriefcommunicationpapersupplementary.pdf